Electronic Supplementary Material (ESI) for Chemical Communications.

Supporting Information

^{19}F-tagged metal binding pharmacophores for NMR screening of metalloenzymes

Kathleen E. Prosser, Alysia J. Kohlbrand, Hyeonglim Seo, Mark Kalaj, Seth M. Cohen*

Department of Chemistry and Biochemistry, University of California, San Diego, 9500 Gilman Drive, La Jolla, CA 92093

*scohen@ucsd.edu

Table of Contents

Compound Characterization

General. Compounds **1**, **2**, **3**, **4**, **5**, **6**, **9**, **10**, **11**, **12**, **1a-4a** and **7a-11a** were purchased from commercial sources (Sigma Aldrich or Combi-Blocks), verified using NMR and used without further purification. Compound **7** has been previously reported and was prepared according to a literature procedure, verified using ^{1}H and ^{19}F NMR.[1] Compound **8** has not been previously reported, and was prepared using the analogous procedure reported for the preparation of the non-fluorinated analogue. The identity of compound **8** was confirmed using ^{1}H, ^{19}F and ^{13}C NMR.[2]

^{19}F-tagged Compound Details:

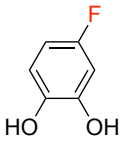

1

4-Fluorobenzene-1,2-diol (**1**). ^{19}F NMR (471 MHz, DMSO-d_6): δ -128.39 (td, J = 9.0, 6.3 Hz). ^{1}H NMR (500 MHz, DMSO-d_6): δ 9.10 (s, 2H), 6.67 (dd, J = 8.7, 5.9 Hz, 1H), 6.53 (dd, J = 10.1, 3.1 Hz, 1H), 6.40 (td, J = 8.6, 3.1 Hz, 1H). ^{13}C NMR (126 MHz, DMSO-d_6): δ 155.48 (d, J = 233.1 Hz), 146.21 (d, J = 11.4 Hz), 141.81 (d, J = 2.4 Hz), 115.45 (d, J = 9.9 Hz), 104.56 (d, J = 22.3 Hz), 102.98 (d, J = 25.5 Hz). ESI-MS: *m/z* 127.28 [M-H]$^{-}$.

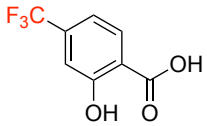

2

2-Hydroxy-4-(trifluoromethyl)benzoic acid (**2**). ^{19}F NMR (471 MHz, DMSO-d_6): δ -62.02. ^{1}H NMR (500 MHz, DMSO-d_6): δ 7.98 (d, J = 8.2 Hz, 1H), 7.29 (s, 1H), 7.25 (d, J = 8.2 Hz, 1H). ^{13}C NMR (126 MHz, DMSO-d_6): δ 170.70, 160.82, 134.69 (q, J = 31.9 Hz), 131.81, 124.47 (q, J = 275.5 Hz), 117.18, 115.41, 114.10. ESI-MS: *m/z* 205.14 [M-H]$^{-}$.

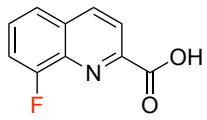

3

8-Fluoroquinoline-2-carboxylic acid (**3**). ^{19}F NMR (471 MHz, DMSO-d_6): δ -126.26 (dd, J = 9.2, 6.2 Hz). ^{1}H NMR (500 MHz, DMSO-d_6): δ 13.63 (s, 1H), 8.67 (d, J = 8.7 Hz, 1H), 8.19 (d, J = 8.7 Hz, 1H), 8.03 (d, J = 8.5 Hz, 1H), 7.88 (td, J = 8.2, 6.1 Hz, 1H), 7.60 (dd, J = 10.0, 7.8 Hz, 1H). ^{13}C NMR (126 MHz, DMSO-d_6): δ 166.54, 157.39 (d, J = 253.8 Hz), 150.23, 147.99 (d, J = 2.7 Hz), 131.15 (d, J = 3.9 Hz), 130.93 (d, J = 9.0 Hz), 126.55 (d, J = 4.0 Hz), 121.73 (d, J = 2.3 Hz), 119.53 (d, J = 16.4 Hz), 112.74 (d, J = 18.8 Hz). ESI-MS: *m/z* 190.14 [M-H]$^{-}$.

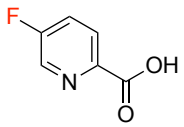

4

5-Fluoropicolinic acid (**4**). ^{19}F NMR (471 MHz, DMSO-d_6): δ -125.52 (d, J = 44.5 Hz). ^{1}H NMR (500 MHz, DMSO-d_6): δ 8.67 (d, J = 2.8 Hz, 1H), 8.12 (dd, J = 8.7, 4.7 Hz, 1H), 7.86 (td, J = 8.7, 2.9 Hz, 1H). ^{13}C NMR (126 MHz, DMSO-d_6): δ 165.81, 161.00 (d, J = 259.5 Hz), 146.28, 138.27 (d, J = 24.3 Hz), 127.24 (d, J = 5.8 Hz), 124.42 (d, J = 18.6 Hz). ESI-MS: *m/z* 140.17 $[M-H]^-$.

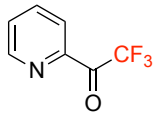

5

2,2,2-Trifluoro-1-(pyridin-2-yl)ethan-1-one (**5**). ^{19}F NMR (471 MHz, DMSO-d_6): δ -86.16. ^{1}H NMR (500 MHz, DMSO-d_6): δ 8.62 (ddd, J = 4.8, 1.8, 1.0 Hz, 1H), 7.93 (td, J = 7.8, 1.7 Hz, 1H), 7.73 (d, J = 7.9 Hz, 1H), 7.49 (ddd, J = 7.5, 4.8, 1.2 Hz, 1H). ^{13}C NMR (126 MHz, DMSO-d_6): δ 156.05, 148.35, 137.89, 125.08, 122.69 (d, J = 1.6 Hz), 92.62 (q, J = 31.0 Hz). ESI-MS: *m/z* 176.26 $[M+H]^+$.

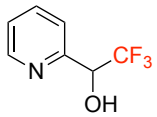

6

2,2,2-Trifluoro-1-(pyridin-2-yl)ethan-1-ol (**6**). ^{19}F NMR (471 MHz, DMSO-d_6): δ -81.37 (d, J = 5.8 Hz). ^{1}H NMR (500 MHz, DMSO-d_6): δ 8.57 (ddd, J = 4.8, 1.8, 0.9 Hz,1H), 7.90 (td, J = 7.7, 1.8 Hz, 1H), 7.61 (d, J = 7.8 Hz, 1H), 7.42 (ddd, J = 7.6, 4.8, 1.2 Hz, 1H), 5.12 (q, J = 7.5 Hz, 1H). ^{13}C NMR (126 MHz, DMSO-d_6): δ 155.64, 149.17, 137.61, 125.22 (q, J = 291.4 Hz), 124.53, 122.58, 72.69 (q, J = 29.9 Hz). ESI-MS: *m/z* 178.20 $[M+H]^+$.

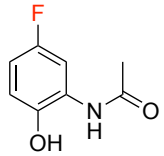

7

N-(5-Fluoro-2-hydroxyphenyl)acetamide (**7**). ^{19}F NMR (471 MHz, DMSO-d_6): δ -120.64 (q, J = 8.7 Hz). ^{1}H NMR (500 MHz, DMSO-d_6): δ 10.26 (s, 1H), 9.28 (s, 1H), 7.63 (dd, J = 8.9, 6.5 Hz, 1H), 6.64 (t, J = 10.1, 3.0 Hz, 1H), 6.58 (td, J = 8.6, 2.9 Hz, 1H), 2.06 (s, 3H).^{13}C NMR (126 MHz, DMSO-d_6): δ 169.30, 159.37 (d, J = 240.0 Hz), 150.13 (d, J = 11.3 Hz), 124.29 (d, J = 10.0 Hz), 123.32 (d, J = 2.9 Hz), 105.42 (d, J = 21.8 Hz), 103.22 (d, J = 24.6 Hz), 23.91. ESI-MS: *m/z* 170.14 $[M+H]^+$.

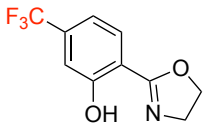

8

2-(4,5-Dihydrooxazol-2-yl)-5-(trifluoromethyl)phenol (**8**). ^{19}F NMR (471 MHz, DMSO-d_6): δ -61.75. ^{1}H NMR (500 MHz, DMSO-d_6): δ 12.68 (s, 1H), 7.84 (d, J = 8.1 Hz, 47H), 7.34 (s, 10H), 7.28 (d, J = 8.1 Hz, 12H), 4.53 (t, J = 9.5 Hz, 52H), 4.12 (t, J = 9.5 Hz, 22H). ^{13}C NMR (126 MHz, DMSO-d_6): δ 165.05 , 159.63 , 133.60 (q, J = 32.0 Hz), 129.57 , 123.90 (q, J = 272.9 Hz), 115.74 (q, J = 3.8 Hz), 114.01, 113.75 (q, J = 3.7 Hz), 67.97 , 53.45. ESI-MS: *m/z* 232.35 $[M+H]^+$.

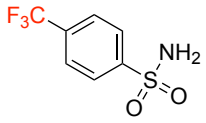

9

4-(Trifluoromethyl)benzenesulfonamide (**9**). ^{19}F NMR (471 MHz, DMSO-d_6): δ -61.38. ^{1}H NMR (500 MHz, DMSO-d_6): δ 8.06 – 7.95 (m, 4H), 7.62 (s, 2H). ^{13}C NMR (126 MHz, DMSO-d_6): δ 148.27 (d, J = 1.5 Hz), 132.13 (q, J = 32.2 Hz), 127.08, 126.76 (q, J = 3.8 Hz), 125.13, 122.96, 120.79. ESI-MS: *m/z* 224.19 $[M-H]^-$.

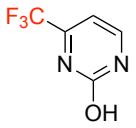

10

4-(Trifluoromethyl)pyrimidin-2-ol (**10**). ^{19}F NMR (471 MHz, DMSO-d_6): δ -70.25. ^{1}H NMR (500 MHz, DMSO-d_6): δ 12.81 (s, 1H), 8.63 – 8.15 (m, 2H), 6.83 (s, 1H). ^{13}C NMR (126 MHz, DMSO-d_6): δ 162.81, 157.32, 153.04, 120.11 (q, J = 277.3 Hz), 99.97. ESI-MS: m/z 163.25 $[M-H]^-$.

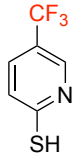

11

5-(Trifluoromethyl)pyridine-2-thiol (**11**). ^{19}F NMR (471 MHz, DMSO-d_6): δ -66.92. ^{1}H NMR (500 MHz, DMSO-d_6): 8.07 (s, 1H), 7.69 – 7.51 (m, 1H), 7.45 – 7.29 (m, 1H). ^{13}C NMR (126 MHz, DMSO-d_6): δ 182.26 (d, J = 11.5 Hz), 137.56, 134.63 (d, J = 11.9 Hz), 132.46, 124.05 (q, J = 269.9 Hz), 114.62 (q, J = 34.7, 11.6 Hz). ESI-MS: *m/z* 180.24 $[M+H]^+$.

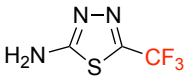

12

5-(Trifluoromethyl)-1,3,4-thiadiazol-2-amine (**12**). ^{19}F NMR (471 MHz, DMSO-d_6): δ -63.74. ^{13}C NMR (126 MHz, DMSO-d_6): δ 172.84, 144.60, 121.92 (q). ESI-MS: *m/z* 170.22 $[M+H]^+$.

NMR Experimental Details

General. All spectra (^{1}H and ^{19}F) were collected on a JOEL ECA 500, Jeol 2 channel inverse-detect $^{1}H/^{19}F$, broad band probe. ^{19}F NMR experiments where set up such that acquisition times were at least 1 s with a total repetition time of at least 3 s. A typical spectrum was collected over 128 scans in approximately 7 min. Aqueous experiments were performed in H_2O 50 mM HEPES buffer pH 8 with a coaxial tube containing 100 µL of a 1 mM solution of trifluoroacetic acid (^{19}F δ = -75.5 ppm) in D_2O. Experiments carried out in buffer were each prepared with 10% DMSO to ensure fragment solubility and a final sample volume of 500 µL. All fragments were prepared and stored as 50 mM stock solutions in DMSO. The linewidths examined in order to determine the change in linewidth in the NMR experiments were evaluated using the line-fitting software in MestReNova (v 14.1.1). In each experiment the percent change in full width at half-maximum (FWHM) linewidth was calculated against a freshly prepared sample containing identical components except for the protein/metal ion of interest.

Preparation of Co(II)-hCAII Metalloform

hCAII sample concentrations were measured using a NanoDrop Instrument (NanoDrop 2000c), which provides the protein concentration in mg/mL. An extinction coefficient of 50,070 M^{-1} cm^{-1} was used.[3] A dialysis tube containing human carbonic anhydrase II (hCAII, 30 mg) in buffer (50 mM HEPES pH 8, 13 mL) was dialyzed for 12 h against 2,6-pyridinedicarboxylic acid (2,6-PDCA) (50 mM 2,6-PDCA in 50 mM HEPES buffer pH 8, 4 L). After which the chelating buffer was replaced with fresh chelating buffer and dialyzed for another 12 h at 4 °C. The tube was removed and dialyzed against buffer (50 mM HEPES pH 8, 4 L) to remove excess 2,6-PDCA. Cobalt was added by dialyzing against $CoCl_2$ (200 eq in 50 mM HEPES pH 8, 2 L) at room temperature. To remove unbound cobalt, the tube was dialyzed against buffer (50 mM HEPES pH 8, 4 L) for 12 h, after which the chelating buffer was replaced with fresh chelating buffer and dialyzed for another 12 h at 4 °C.

Samples were prepared for ICP-MS analysis by dissolving 50 ppm protein in 100 uL of concentrated nitric acid (trace grade), with each sample then diluted to a 10 mL, 1% nitric acid solution in MiliQ ultrapure water. All experiments were performed on an iCAP RQ ICP-MS instrument and Qtegra analysis software was used for data processing. The ratio between Zn- and Co-hCAII populations in each sample was calculated based on the total metal concentration determined by ICP-MS. Co-substituted samples were found to be 90% Co and 10% Zn and apo protein samples contained less than 10 ppb (0.05 molar equivalence) Zn.

Compound 9 Titration with hCAII

Compound **9** was diluted to final sample concentrations of 500 µM and individual samples were prepared with 0, 0.02, 0.05, 0.1, 0.2, 0.5, and 1 equiv of hCAII. A second titration as carried out with 200 µM **9** and 0.02, 0.05, 0.1, and 0.2 equiv of hCAII to validate the observations at lower concentrations.

Screening Experiments with hCAII and BSA

Stock solutions of each ^{19}F-tagged MBP were diluted into a master mix with a concentration of 4 mM for each fragment. Master mixes comprised all 12 compounds, **1**,

3, **6**, **9**, **11**, and **12**, or **2**, **4**, **5**, **7**, **8**, and **10** in DMSO. Each master mix was then diluted to a final concentration of 400 μM into samples containing buffer, hCAII (80 μM) or bovine serum albumin (BSA, 80 μM).

Acetazolamide Competition Experiment

Compound **9** was diluted in buffer to a final concentration of 300 μM. Control samples containing no protein and no acetazolamide were prepared, as well as five samples contained 100 μM hCAII and 0, 3 nM, 30 nM, 3 μM, or 300 μM acetazolamide.

Co(II)-hCAII and $CoCl_2$ Titrations

A sample of Co(II)-hCAII was prepared as described above and isolated as a 1.64 mg/mL (55.7 μM) solution in HEPES buffer. Compound **9** was diluted to give a final concentration of 200 μM fragment, and in five individual samples was added the Co(II)-hCAII solution or buffer to give 0, 0.02, 0.05, 0.1 and 0.2 equiv of protein. A control experiment was performed using $CoCl_2$, where a 200 μM solution of fragment **9** was incubated with 0, 0.02, 0.05 or 0.1 equivalents of $CoCl_2$ in 50 mM HEPES at pH 8 and examined using ^{19}F NMR.

Table S1. ^{19}F NMR chemical shift for each of the fluorinated fragments in DMSO-d_6 and in H_2O HEPES buffer (50 mM HEPES, pH 8).

	^{19}F NMR Chemical Shift (ppm)	
Compound	DMSO	HEPES Buffer (10% DMSO)
1	-128.39	-123.37
2	-62.02	-62.59
3	-126.26	-122.10
4	-125.52	-123.72
5	-86.16	-82.97
6	-81.37	-76.86
7	-120.64	-113.94
8	-61.75	-63.00
9	-61.38	-62.57
10	-70.25	-70.07
11	-66.92	-61.78
12	-63.74	-59.75

Table S2. Percent change in the observed FWHM linewidth for compound **9** when incubated with Zn(II)-hCAII, apo protein, $CoCl_2$, or Co(II)-hCAII. The error values are standard deviations based on three replicate experiments.

	Percent change in ^{19}F NMR FWHM with Compound **9**				
Equivalents	Zn(II)-hCAII (500 μM **9**)	Zn(II)-hCAII (200 μM **9**)	Apo hCAII (200 μM **9**)	$CoCl_2$ (200 μM **9**)	Co(II)-hCAII (200 μM **9**)
0.02	2%	1 ± 1%	-	-	1 ± 1%
0.05	2%	2 ± 3%	0%	2 ± 1%	4 ± 2%
0.1	6%	5 ± 1%	3%	3 ± 2%	8 ± 1%
0.2	8%	8 ± 1%	5%	6 ± 2%	13 ± 2%
0.5	28%	-	9%	-	-
1	95%	-	-	-	-

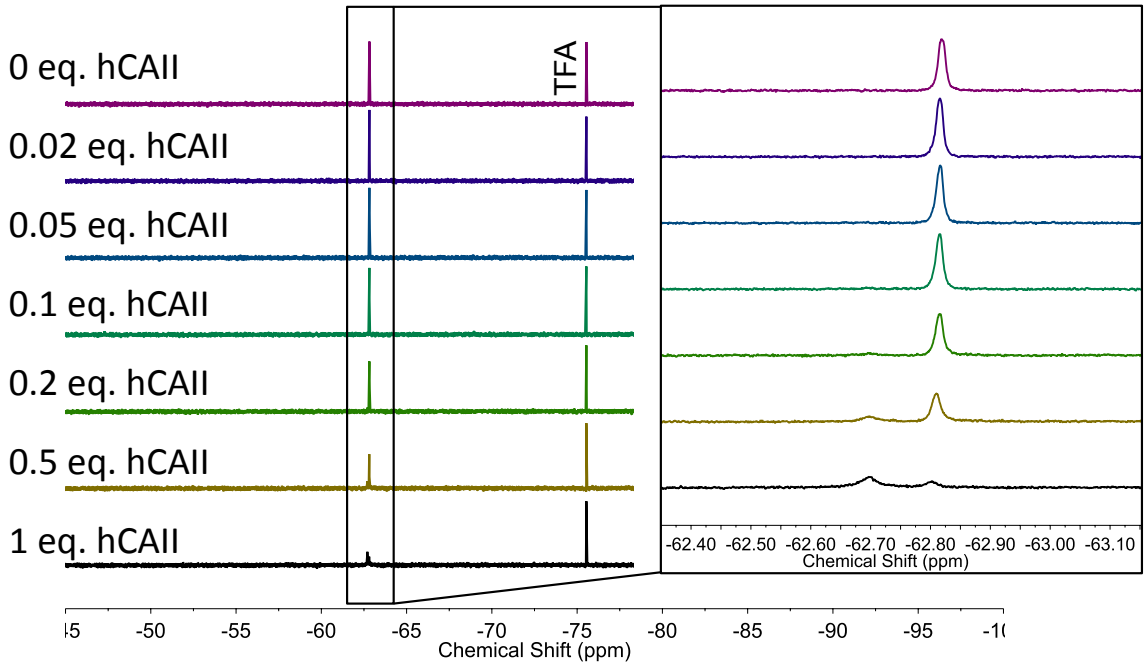

Figure S1. ^{19}F NMR titration of compound **9** (500 µM) with Zn(II)-hCAII, from 0 to 1 equivalent in 50 mM HEPES buffer pH 8.

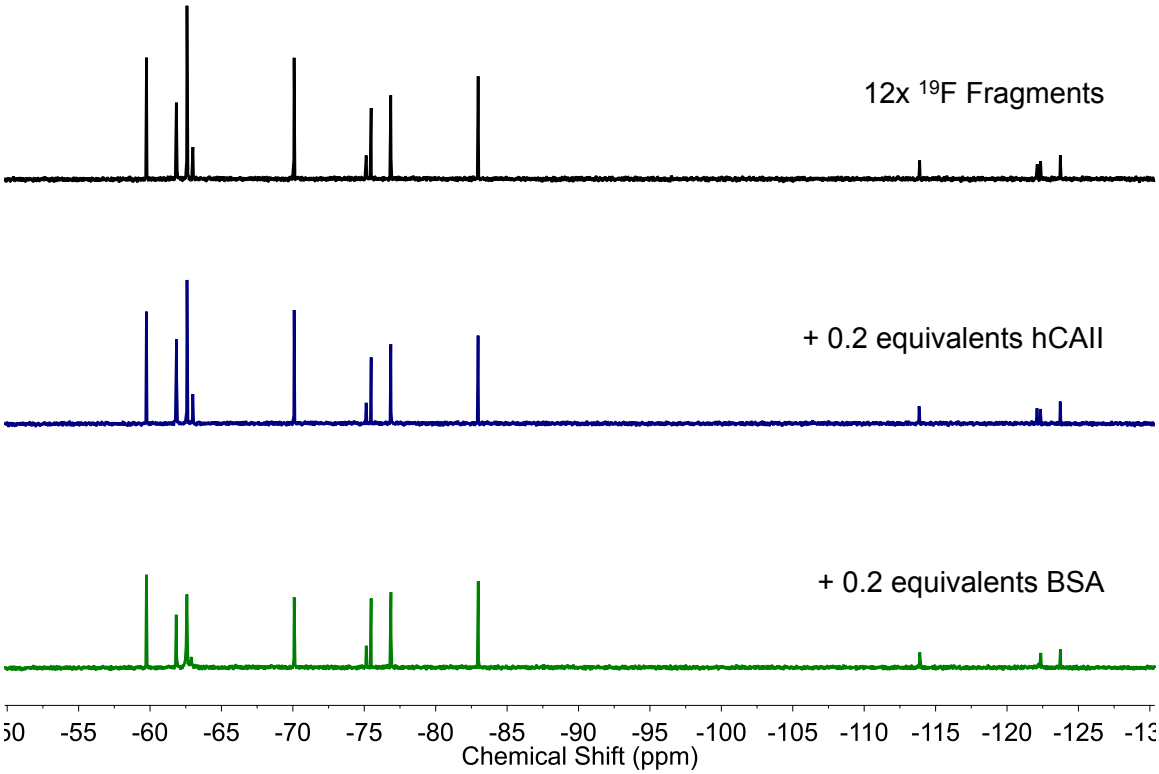

Figure S2. ^{19}F NMR spectra of the twelve ^{19}F-tagged MBPs (400 μM) in 50 mM HEPES buffer pH 8 with no protein, 80 μM Zn(II)-hCAII, and 80 μM bovine serum albumin (BSA).

Table S3. Percent change in the observed FWHM linewidth for ^{19}F-tagged fragments incubated with Zn(II)-hCAII or BSA (0.2 equiv).

	Percent change in ^{19}F NMR FWHM			
Fragment	Zn(II)-hCAII (12 fragments)	BSA (12 fragments)	Zn(II)-hCAII (6 fragments)	Zn(II)-hCAII (6 fragments)
12	0%	13%	-	4%
11	11%	70%	-	21%
9 & 2	15%	133%	-	-
9	-	-	-	29%
2	-	-	7%	-
8	1%	227%	2%	-
10	6%	23%	0%	-
6	3%	5%	-	8%
5	5%	12%	6%	-
7	1%	15%	4%	-
3	5%	233%	-	3%
1	0%	3%	-	0%
4	1%	26%	5%	-

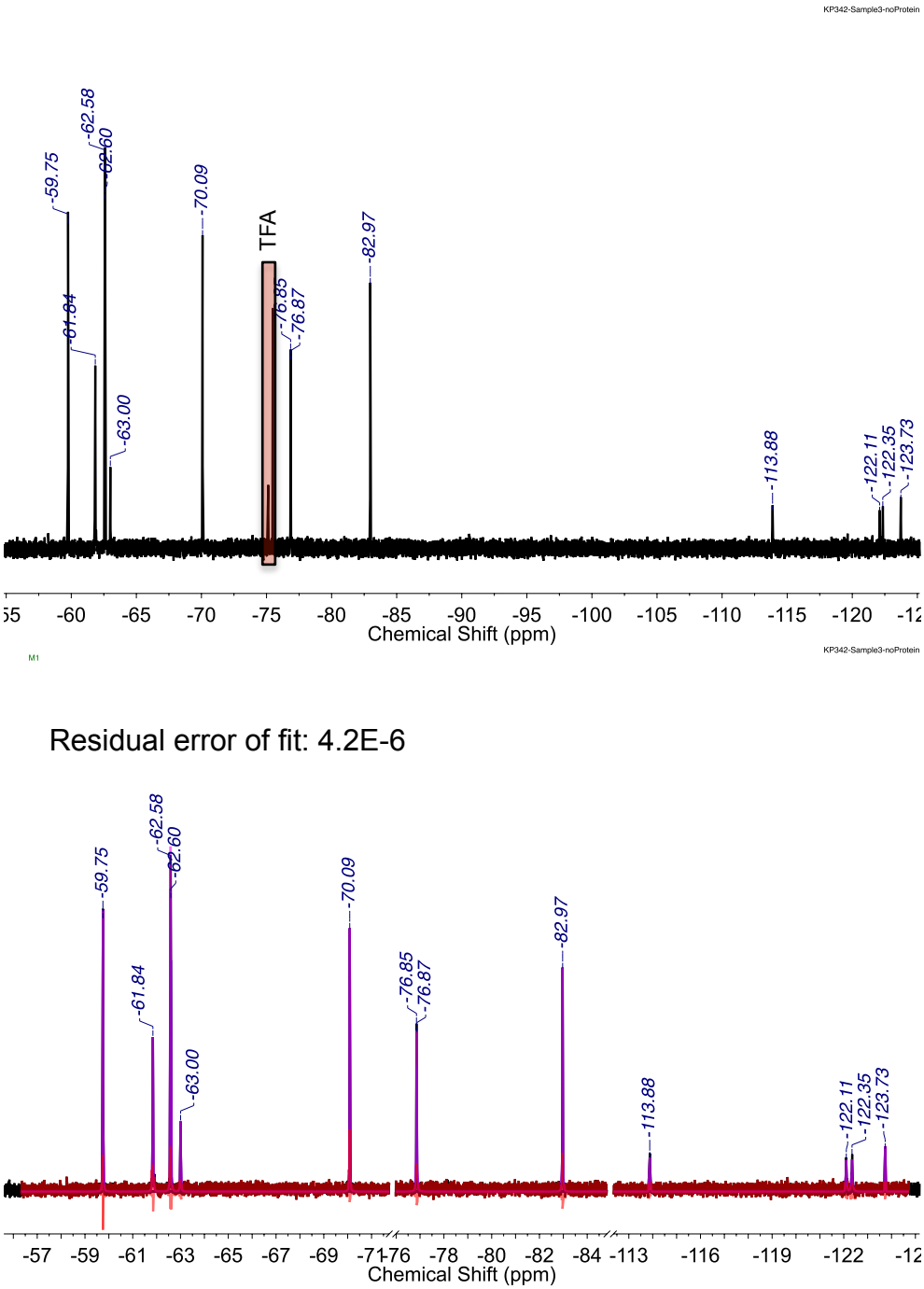

Figure S3. A representative example of the line-fitting performed in MestReNova. *Top*: ^{19}F NMR spectra of the twelve ^{19}F-tagged MBPs (400 μM) in 50 mM HEPES buffer (pH 8) with no protein. *Bottom*: The sample spectrum (black) overlaid with the fit line (purple) and the residual line (red).

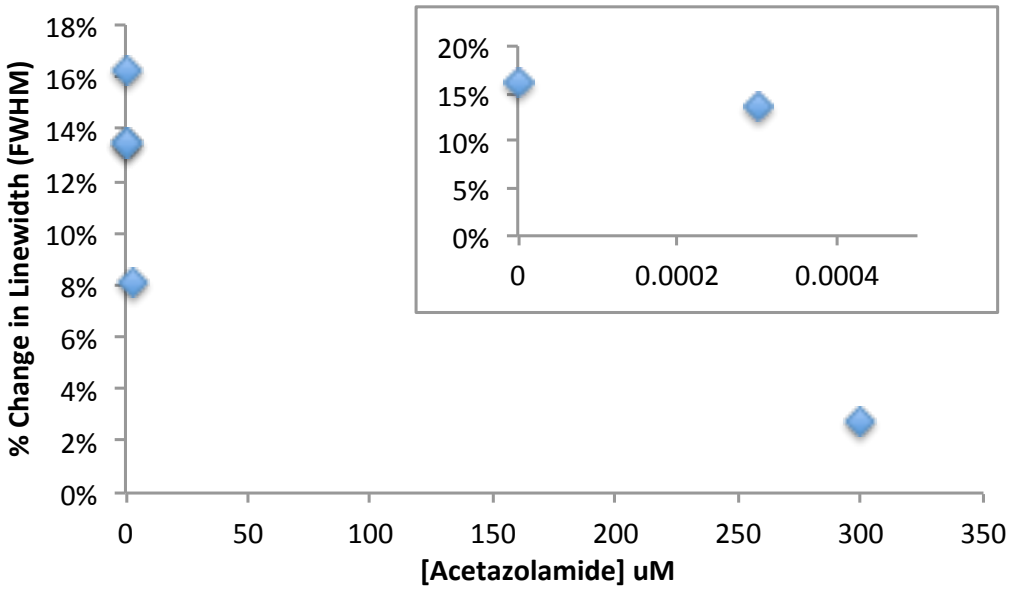

Figure S4. The percent change in the ^{19}F NMR resonance FWHM of compound **9** (300 µM) incubated with 100 µM Zn(II)-hCAII in the presence of acetazolamide (0-1 equivalents).

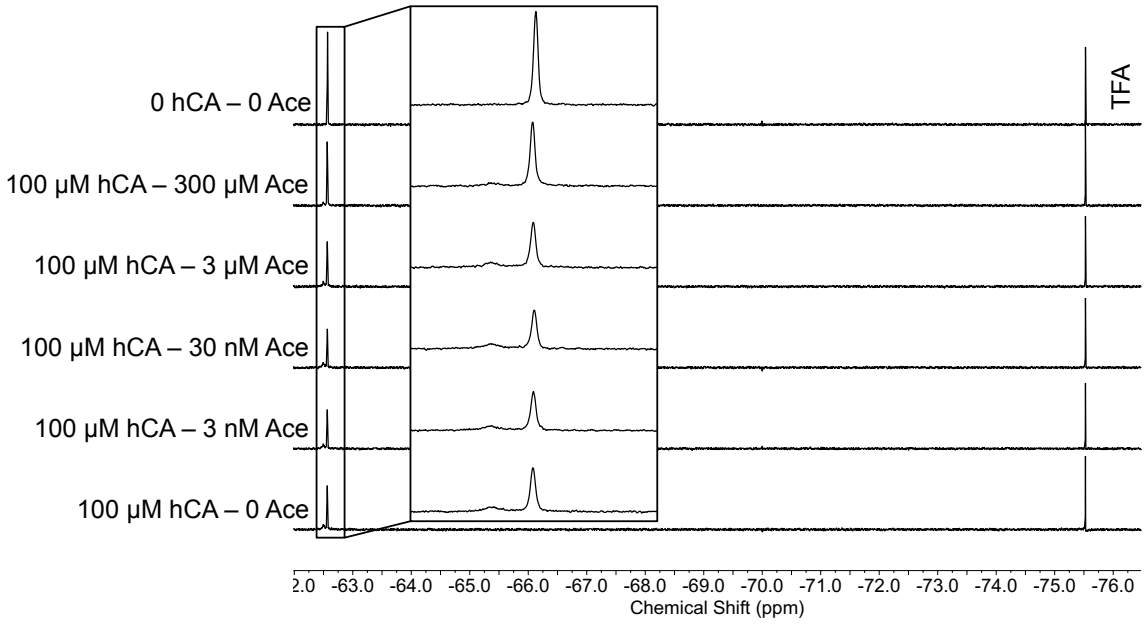

Figure S5. The ^{19}F NMR spectra of compound **9** (300 µM) incubated with no protein or 100 µM Zn(II)-hCAII in the presence of acetazolamide (0-1 equivalents). The addition of acetazolamide outcompetes compound **9** for the hCAII active site and restores the intensity and linewidth of the primary peak at -62.6 ppm.

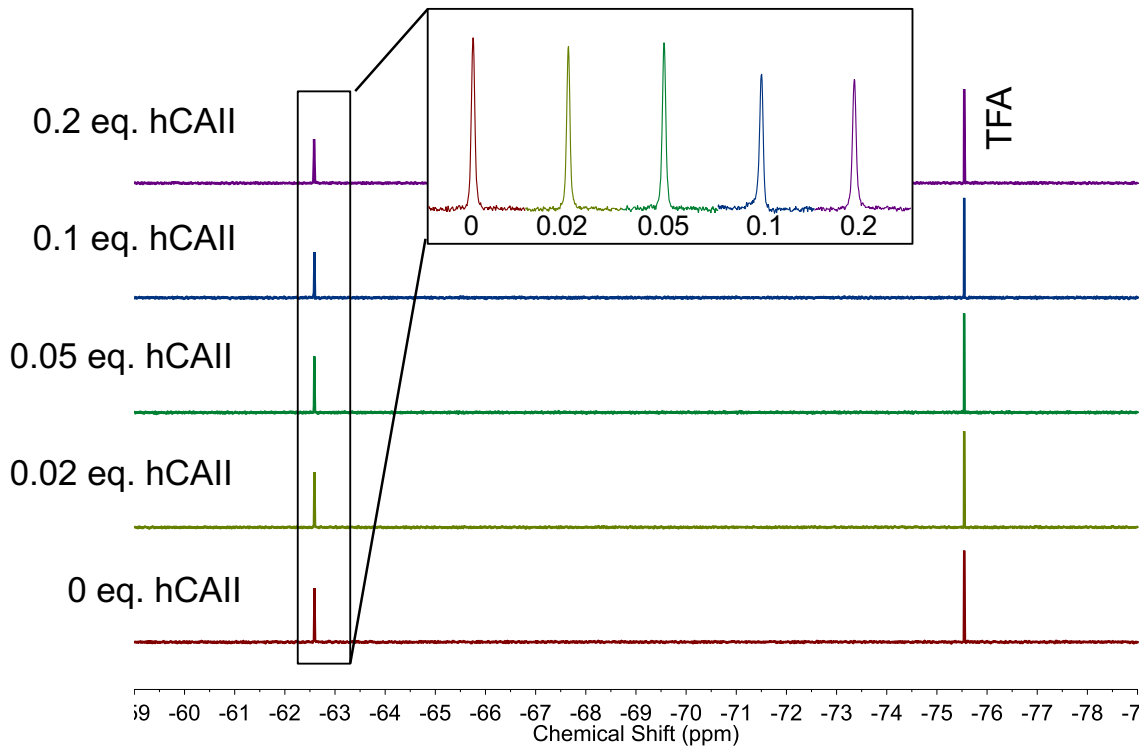

Figure S6. The ^{19}F NMR spectra of fragment **9** (200 μM) in 50 mM HEPES buffer pH 8 with no protein or Co(II)-hCAII (0-40 μM).

Colorimetric hCAII Activity Assays

hCAII was expressed and purified as previously described.[4] Assays were carried out in clear Costar 96-well plates. Wells were prepared to a final volume of 100 μL including buffer (50 mM HEPES, pH 8.0), hCAII (40 nM), inhibitor (100 μM), and *p*-nitrophenyl acetate (500 μM). The inhibitor and protein were preincubated for 10 min at 30 °C and *p*-nitrophenol was added to the reaction mixture immediately before reading. The change in absorbance at 405 nm was monitored for 20 min and the rates of the reaction over the first 15 min were determined. Readings from background wells containing no protein were subtracted from the active assay wells in order to eliminate the effects of substrate background hydrolysis not cause by hCAII. By comparing to control well with substrate and protein only, percent inhibition of the protein by fragments was determined.

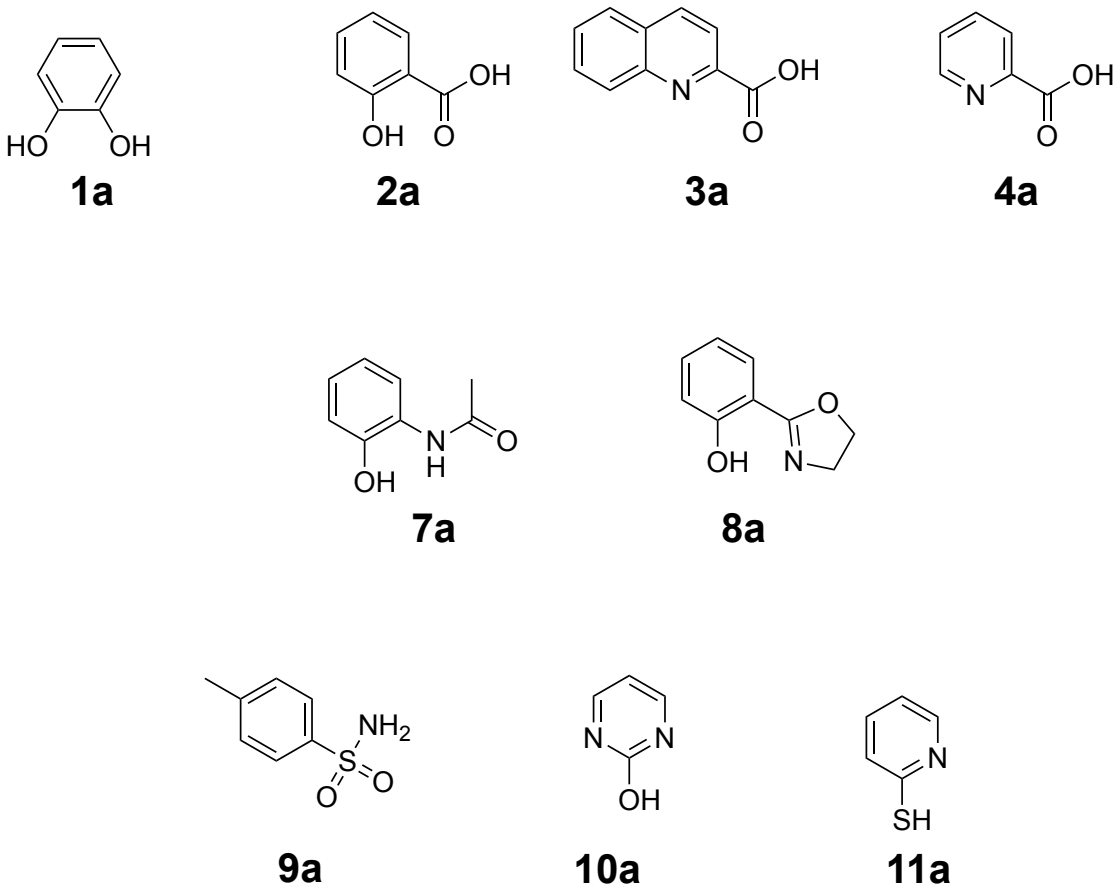

Figure S7. Non-fluorinated analogues for several of the ^{19}F-tagged MBPs.

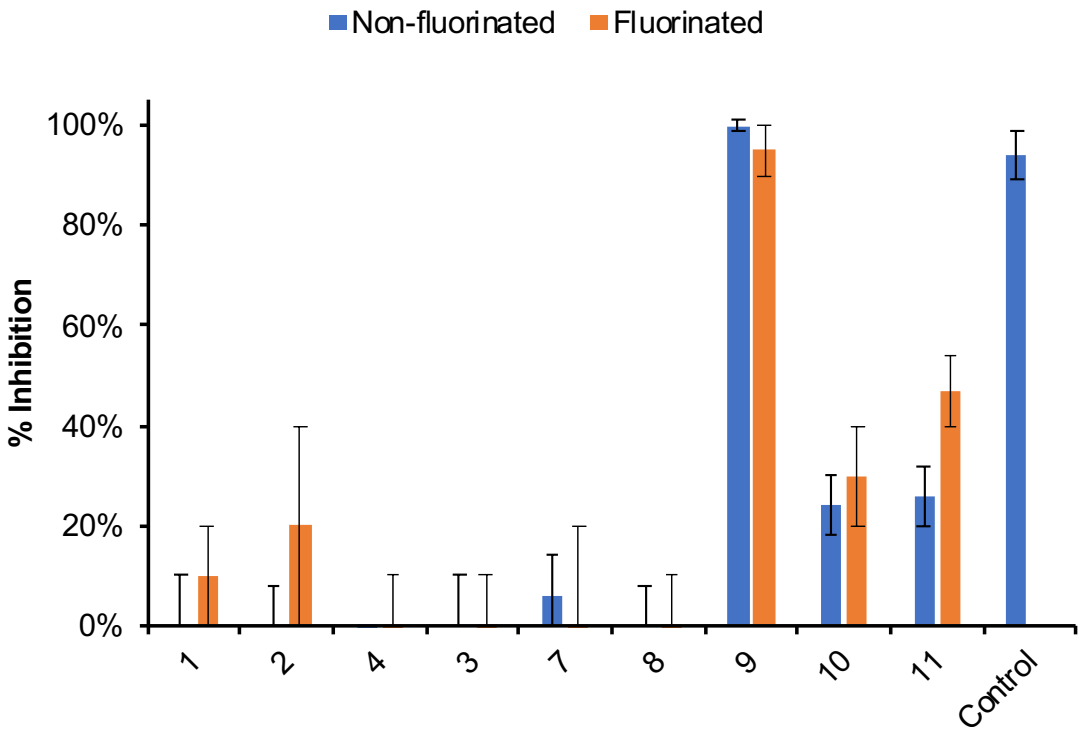

Figure S8. Comparison of the percent inhibition of hCAII by fluorinated and non-fluorinated fragments at a concentration of 100 μM. The control used here is acetazolamide.

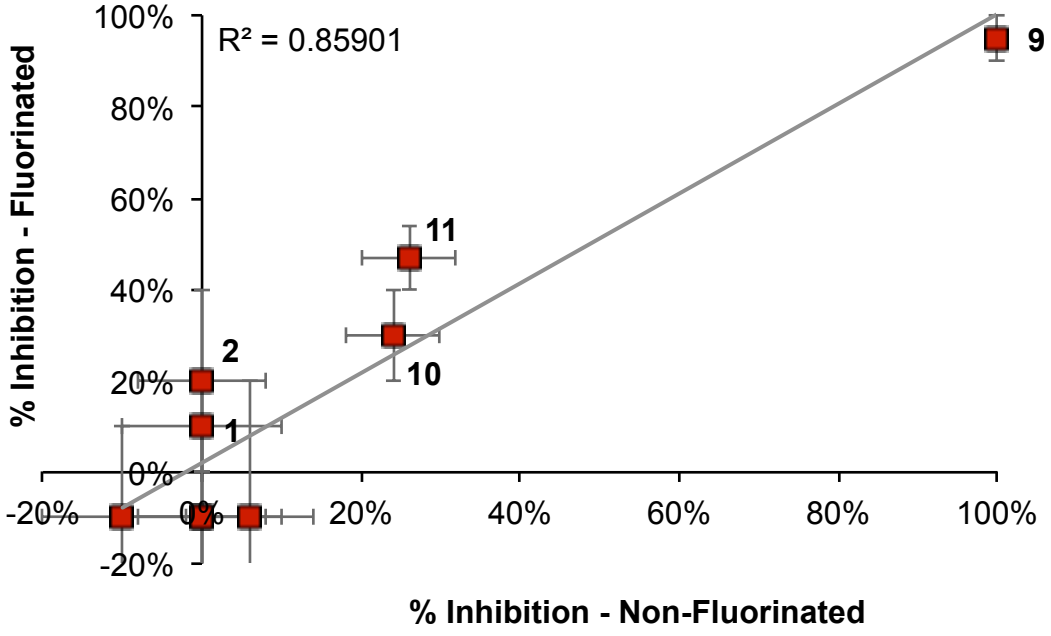

Figure S9. Correlation plot of the percent inhibition of hCAII by the non-fluorinated and the fluorinated fragments.

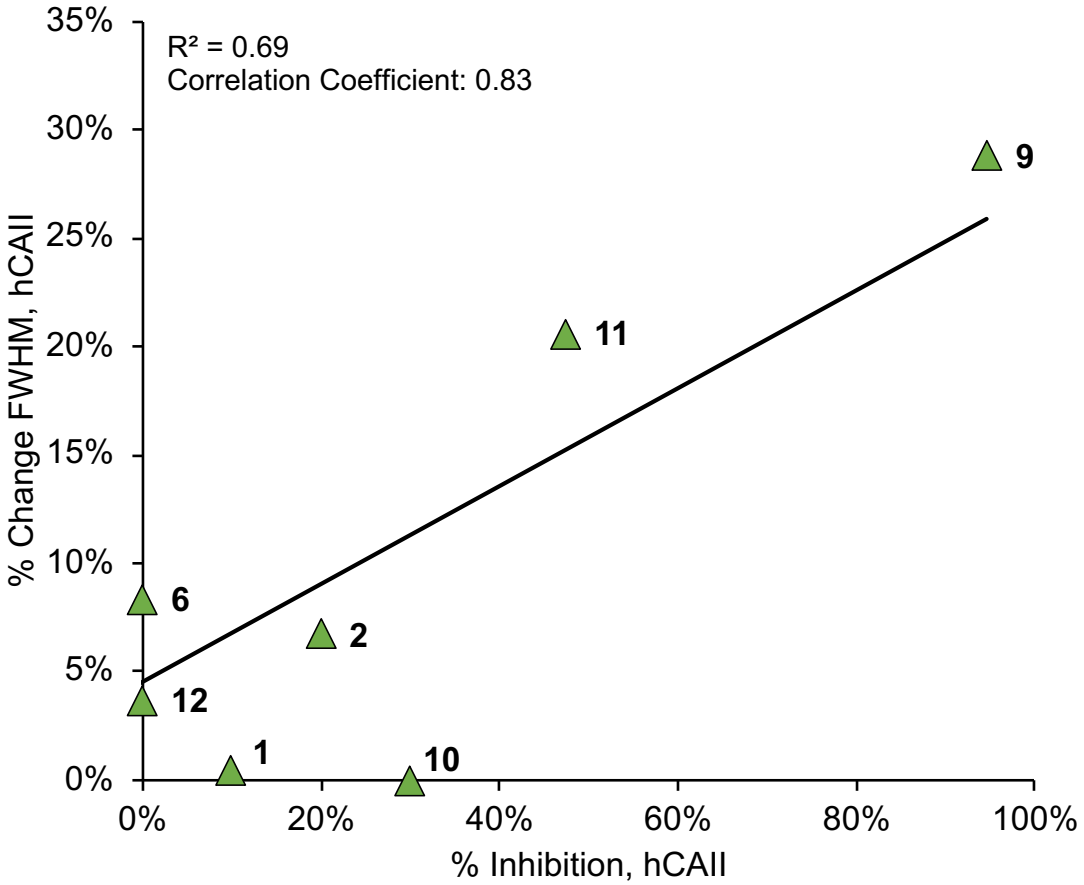

Figure S10. Correlation plot of the percent inhibition caused by the ^{19}F-tagged MBPs in the hCAII colorimetric assay against the percent change in ^{19}F NMR resonance linewidth when those compounds were incubated with hCAII.

X-ray Crystallography

[($Tp^{Ph,Me}$)ZnOH] ($Tp^{Ph,Me}$= hydrotris(5,3-methylphenylpyrazolyl)borate)) was prepared according to a literature procedure.[5] [($Tp^{Me,Ph}$)$_2$Zn(**4**)], [($Tp^{Me,Ph}$)$_2$Zn(**9**)], and [($Tp^{Me,Ph}$)$_2$Zn(**9a**)] were prepared using a procedure reported for the preparation of other [($Tp^{Me,Ph}$)Zn(MBP)] complexes.[6] The products were crystallized as colorless blocks from a solution of benzene diffused with pentanes. Suitable crystals were selected and data was collected at 100 K on a Bruker APEX-II Ultra diffractometer with a Mo-Kα Microfocus Rotating Anode and a APEX-II CCD area detector or a Bruker Kappa diffractometer equipped with a Bruker X8 APEX II Mo sealed tube and a Bruker APEX-II CCD. The data was integrated and merged within the APEXIII software suite (Bruker, 2017). The structure was refined with the XL[7] refinement package using least squares minimization using Olex2.[8] The crystal data file of all complexes was deposited into the Cambridge Crystallographic Data Centre (CCDC). Crystallographic data collection and refinement information is listed in Table S4. Disordered solvent was treated with the PLATON SQUEEZE[9] function in complex **9**.

Table S4. Crystal data and structure refinement for [(TpPh,Me)Zn(MBP)] complexes.

Compound	[($Tp^{Ph,Me}$)Zn(**4**)]	[($Tp^{Ph,Me}$)Zn(**9**)]	[($Tp^{Ph,Me}$)Zn(**9a**)]
Identification code	2036941	2036942	2036943
Empirical formula	$C_{36}H_{31}BFN_7O_2Zn$	$C_{37}H_{33}BF_3N_7O_2SZn$	$C_{40}H_{38}BN_7O_2SZn$
Formula weight	688.86	772.94	757.01
Temperature/K	100	100	100
Crystal system	triclinic	trigonal	monoclinic
Space group	P-1	R-3	$P2_1/c$
a/Å	11.6354(9)	33.345(4)	12.5509(14)
b/Å	11.6529(9)	33.345(4)	12.1199(12)
c/Å	11.9411(9)	17.251(3)	23.821(3)
α/°	87.746(2)	90	90
β/°	83.9050(10)	90	96.616(4)
γ/°	89.1230(10)	120	90
Volume/$Å^3$	1608.5(2)	16612(4)	3599.5(7)
Z	2	18	4
$\rho_{calc}g/cm^3$	1.422	1.391	1.397
μ/mm^{-1}	0.815	0.78	0.787
F(000)	712	7164	1576
Crystal size/mm^3	0.2 × 0.2 × 0.1	0.2 × 0.1 × 0.1	0.1 × 0.1 × 0.1
Radiation	MoKα (λ = 0.71073)	MoKα (λ = 0.71073)	MoKα (λ = 0.71073)
2Θ range for data collection/°	3.432 to 52.16	2.442 to 52.872	3.776 to 52.912
Index ranges	$-14 \le h \le 13$, $-14 \le k \le 10$, $-14 \le l \le 14$	$-41 \le h \le 41$, $-41 \le k \le 36$, $-21 \le l \le 21$	$-15 \le h \le 15$, $-15 \le k \le 14$, $-29 \le l \le 29$
Reflections collected	10474	66804	67973
Independent reflections	6361 [R_{int} = 0.0209, R_{sigma} = 0.0410]	7604 [R_{int} = 0.0729, R_{sigma} = 0.0410]	7383 [R_{int} = 0.0855, R_{sigma} = 0.0430]
Data/restraints/parameters	6361/0/436	7604/0/476	7383/0/473
Goodness-of-fit on F^2	1.042	1.03	1.129
Final R indexes [I>=2σ (I)]	R_1 = 0.0354, wR_2 = 0.0777	R_1 = 0.0392, wR_2 = 0.0906	R_1 = 0.0707, wR_2 = 0.1548
Final R indexes [all data]	R_1 = 0.0477, wR_2 = 0.0830	R_1 = 0.0585, wR_2 = 0.0995	R_1 = 0.0866, wR_2 = 0.1630
Largest diff. peak/hole / e $Å^{-3}$	0.67/-0.31	1.57/-0.66	2.01/-1.08

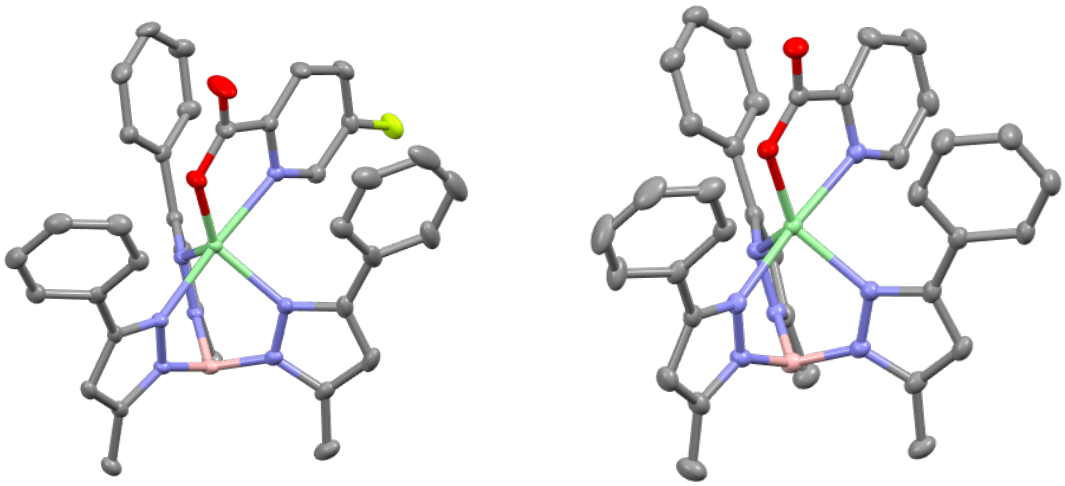

Figure S11. Structure of [(Tp^{Ph,Me})Zn(**4**)] (*left*) and [(Tp^{Ph,Me})Zn(**4a**)] (*right*) (ORTEP, 50% probability ellipsoids).[10] Solvent molecules and hydrogen atoms have been omitted for clarity. Color scheme: carbon = gray, oxygen = red, nitrogen = blue, boron = pink, zinc = green, and fluorine = lime.

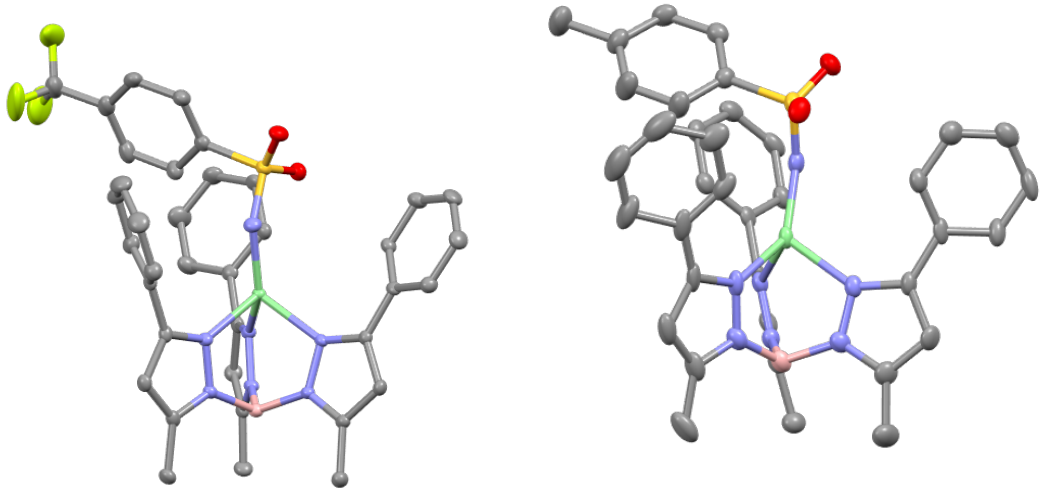

Figure S12. Structure of [(Tp^{Ph,Me})Zn(**9**)] (*left*) and [(Tp^{Ph,Me})Zn(**9a**)] (*right*) (ORTEP, 50% probability ellipsoids). Solvent molecules and hydrogen atoms have been omitted for clarity. Color scheme: carbon = gray, oxygen = red, nitrogen = blue, boron = pink, zinc = green, fluorine = lime, and sulfur = yellow.

Table S5. Selected Bond Lengths and Angles for [(Tp^{Ph,Me})Zn(**4**)] and [(Tp^{Ph,Me})Zn(**4a**)].

	Bond Lengths/Å		Bond Angles/°	Geometry index (τ)
	Zn1-N7	Zn1-O1	N7-Zn1-O1	
4	2.2164(17)	1.95065 (15)	78.69(6)	0.71
4a	2.1745 (15)	1.9645 (12)	79.68(5)	0.72

Table S6. Selected Bond Lengths and Angles for [(Tp^{Ph,Me})Zn(**9**)] and [(Tp^{Ph,Me})Zn(**9a**)].

	Bond Lengths/Å		Bond Angles/°	Geometry index (τ)
	S1-N7	Zn1-N7	S1-N7-Zn1	
9	1.572(3)	1.910(3)	136.4(2)	0.66
9a	1.581(5)	1.924(4)	134.9(3)	0.63

Thermal Shift Assay

Thermal shift assays were performed according to a literature procedure.[11] In brief, in the wells of a 96-well 0.2 mL optical MicroAmp (ThermoFisher) thermocycler plate, 9.5 µL of buffer, 4 µL of hCAII (prepared as described above in 50 mM HEPES buffer, pH 8), 4 µL of inhibitor in buffer (1 mM inhibitor; 10% DMSO), and 2.5 µL of 20′ sypro orange Thermal Shift® dye (ThermoFisher) were mixed. This results in a final well volume of 20 µL containing final concentrations of ~2 µg protein, 200 µM inhibitor, and 6× dye in buffer with 2% DMSO. Thermocycler plate wells were sealed prior to analysis, and the plate was then heated in a thermocycler from 25 °C to 99 °C at a ramp rate of 0.1 °C/sec. Fluorescence was read using the ROX filter channel (λ_{ex} = 580 nm; λ_{em} = 623 nm), and the fluorescence signal was fitted to a first derivative curve to identify T_M.

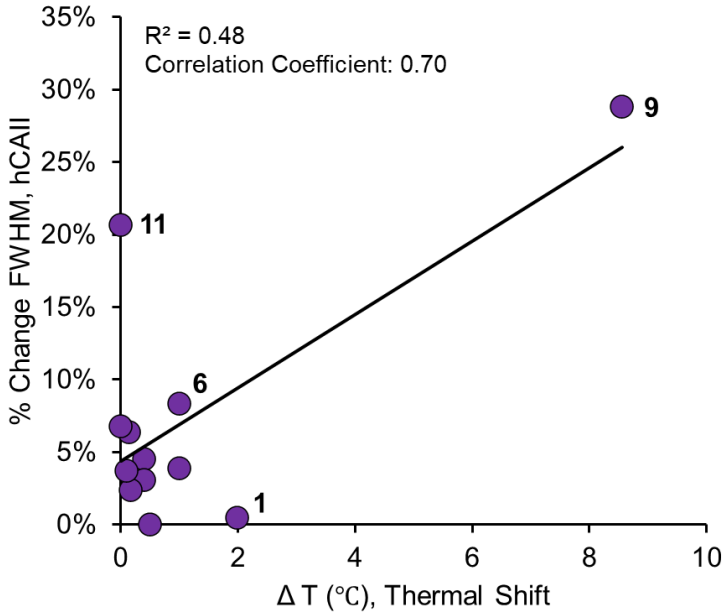

Figure S13. Correlation plot of the thermal shift caused by the ^{19}F-tagged MBPs in the hCAII fluorometric assay against the percent change in ^{19}F NMR resonance linewidth when those compounds were incubated with hCAII.

References

1. Moreno-Corral, R.; Höpfl, H.; Machi-Lara, L.; Lara, K. O., Synthesis, Structural Characterization and Metal Inclusion Properties of 18-, 20- and 22-Membered Oxaazacyclophanes and Oxaazacalix[4]arene Analogues: Macrocyclic Amine and Schiff Base Receptors with Variable NxOy Donor Sets. *Eur. J. Org. Chem.* **2011,** *2011* (11), 2148-2162.
2. Peterson, T.; Falk, K. E.; Leong, S. A.; Klein, M. P.; Neilands, J. B., Structure and behavior of spermidine siderophores. *J. Am. Chem. Soc.* **1980,** *102* (26), 7715-7718.
3. Nair, S. K.; Calderone, T. L.; Christianson, D. W.; Fierke, C. A., Altering the mouth of a hydrophobic pocket. Structure and kinetics of human carbonic anhydrase II mutants at residue Val-121. *J. Biol. Chem.* **1991,** *266*, 17320-17325.
4. Monnard, F. W.; Heinisch, T.; Nogueira, E. S.; Schirmer, T.; Ward, T. R., Human Carbonic Anhydrase II as a host for piano-stool complexes bearing a sulfonamide anchor. *Chem. Commun.* **2011,** *47* (29), 8238-8240.
5. Puerta, D. T.; Cohen, S. M., [(TpMe,Ph)2Zn2(H3O2)]ClO4: a new H3O2 species relevant to zinc proteinases. *Inorganica Chimica Acta* **2002,** *337*, 459-462.
6. Dick, B. L.; Cohen, S. M., Metal-Binding Isosteres as New Scaffolds for Metalloenzyme Inhibitors. *Inorg Chem* **2018,** *57* (15), 9538-9543.
7. Sheldrick, G., A short history of SHELX. *Acta Crystallographica Section A* **2008,** *64* (1), 112-122.
8. Dolomanov, O. V.; Bourhis, L. J.; Gildea, R. J.; Howard, J. A. K.; Puschmann, H., OLEX2: a complete structure solution, refinement and analysis program. *Journal of Applied Crystallography* **2009,** *42* (2), 339-341.
9. Spek, A., PLATON SQUEEZE: a tool for the calculation of the disordered solvent contribution to the calculated structure factors. *Acta Crystallographica Section C* **2015,** *71* (1), 9-18.
10. Jacobsen, F. E.; Lewis, J. A.; Cohen, S. M., A New Role for Old Ligands: Discerning Chelators for Zinc Metalloproteinases. *J. Am. Chem. Soc.* **2006,** *128* (10), 3156-3157.
11. Morrison, C. N.; Prosser, K. E.; Stokes, R. W.; Cordes, A.; Metzler-Nolte, N.; Cohen, S. M., Expanding medicinal chemistry into 3D space: metallofragments as 3D scaffolds for fragment-based drug discovery. *Chem. Sci.* **2020,** *11* (5), 1216-1225.